vessels.[3] Porphyria cutanea tarda is commonly associated with HCV infection, and other disorders have been loosely associated with the virus, including secondary Sjögren's syndrome, Moorhen's corneal ulcer, hyper- and hypothyroidism, and myositis.[4,5] The pathogenesis of these extrahepatic complications is not well understood.[6]

The myocardium is involved in a variety of viral infections. Myocarditis may be the primary disorder or may be part of a systemic disease. Enteroviruses, coxsackievirus B in particular,[7] adenovirus,[8] and parvovirus,[9,10] have been most often implicated in myocarditis. However, despite extensive laboratory investigations, a suspected viral etiology of clinically overt myocarditis often remains unconfirmed, the evidence is only circumstantial, and a direct irrefutable proof of cardiac involvement is not established.[11–13] On the other hand, a link between viral myocarditis and the eventual development of dilated cardiomyopathy is becoming more and more apparent.[14–16]

The importance of HCV in patients with myocarditis and dilated cardiomyopathy has recently been noted.[17–22] In pursuit of this observation, this study was performed to examine the prevalence of HCV infection among patients enrolled in the Myocarditis Treatment Trial,[23] and to see whether myocarditis with HCV infection was associated with biomarkers of myocardial injury.

Patient Population and Methods

The design of the trial, methods of random treatment assignments, patient characteristics, and histopathologic techniques used to diagnose myocarditis have been described previously.[23,24] Briefly, consenting patients were eligible to enter the trial if they had (1) suffered from heart failure of undetermined etiology for up to 2 years, (2) an ejection fraction below 45% by radionuclide left ventriculography, (3) myocarditis proven by endomyocardial biopsy, and (4) no contraindications to immunosuppressive therapy. Endomyocardial biopsy was performed by standard techniques according to local institutional practices, and the specimens were fixed in formalin before being processed, sectioned, and stained with hematoxylin and eosin. The initial histopathologic diagnosis of myocarditis was made at each enrolling institution. The biopsy samples was then reviewed by a panel of 7 expert pathologists, and the diagnosis of myocarditis was confirmed according to the Dallas criteria.[25] The Institutional Review Boards had approved, and study participants agreed to, the investigative use of all biopsy and blood specimens.

Analyses of Anti-HCV Antibody, HCV RNA, HCV Grouping, and Cardiac Troponins I and T, and N-Terminal Pro-Brain Natriuretic Peptide

Sera from 1,355 patients were available among 2,233 enrolled. Anti-HCV antibody was measured by AxSYM HCV Dynapack-II (Abbott Laboratories, Abbott Park, IL). HCV RNA was quantified by AMPLICOR (Roche Molecular Systems, Inc., Pleasanton, CA). HCV grouping was performed by polymerase chain reaction assay.[26] Circulating cardiac troponin I was measured by AxSYM Troponin I (Abbott Laboratories). A cardiac troponin I equal to or above 2.0 ng/ml was defined as abnormal. Cardiac troponin T and N-terminal pro-brain natriuretic peptide (NT-proBNP) were measured by Elecsys (Roche Diagnostics, Tokyo, Japan).

Statistical Analysis

The chi-square test was applied to examine qualitative differences. Student's *t*-test was used for comparisons of quantitative variables. Linear regression analysis was performed for comparisons between cardiac troponins I and T. Values are expressed as means ± standard error. A P value $<.05$ indicates statistical significance.

Results

Anti-HCV antibodies were present in 59 of 1355 patients (4.4%), including 6 of 102 patients (5.9%) with biopsy-proven myocarditis, and 53 of 1253 patients (4.2%) whose biopsy specimens did not satisfy the Dallas criteria (Table 1). This prevalence of HCV infection was higher than that estimated by the Centers for Disease Control and Prevention (1.8%) in the general US population ($P < .01$).[2] The widely variable prevalence of positive HCV antibody among medical centers, between 0% and 15.4%, is shown in Table 2.

Among 59 patients with HCV antibody, HCV genomes were found in the sera of 29 patients (49%). Group 1 HCV was detected in 23, group 2 in 1, and unclassifiable HCV in 5 patients. The mean concentration of circulating HCV was 159 ± 37 kU/mL (range 1–800 kU/mL, Table 3). Cardiac troponin I concentrations, measured in the sera of patients with positive HCV antibody (Table 3) were greater than 2.0 ng/mL in 17 of 56 patients (30%), and cTnT was detectable (≥0.01 ng/mL) in 28 of 59 patients (48%) with HCV antibodies, suggesting the persistence of ongoing myocardial injury. A positive correlation was found between circulating concentrations of cTnI and cTnT ($y = 37x + 0.084$, $r^2 = 0.59$, $P < .0001$). We also measured cardiac troponins I and T in the sera from 50 randomly selected patients presenting with myocarditis without HCV antibody. Cardiac troponin I tended to be higher in patients with than patients without HCV antibody (1.9 ± 0.6 versus 1.4 ± 0.2 ng/mL, $P = .2$). Cardiac troponin T was slightly higher in patients with, than in patients without HCV infection (0.047 ± 0.013 versus 0.039 ± 0.013, $P = .55$), though the difference was not statistically

Table 1. Prevalence of Hepatitis C Virus Infection in the Myocarditis Treatment Trial

Myocarditis	Positive/Total (Number of Patients)	Frequency
Present	6/102	5.9%*
Absent	53/1253	4.2%†
Total	59/1355	4.4%‡

Comparison with prevalence of 1.8% in the general US population (n = 21,241).[2]
*Chi-square = 9.5, $P < .01$.
†Chi-square = 36.9, $P < .001$.
‡Chi-square = 43.5, $P < .001$.

Table 2. Prevalence of Hepatitis C Virus Infection at Individual Institutions Participating in the Myocarditis Treatment Trial

	Total		Myocarditis			
			Present		Absent	
Institution	+/Total	%	+/Total	%	+/Total	%
Beth-Israel Medical Center, New York	2/13	15.4	1/1	100.0	1/12	8.3
University of Cincinnati	6/64	9.5	1/4	25.0	5/60	8.3
University of Connecticut, Farmington	10/107	9.4	0/5	0.0	10/102	8.7
University of Tennessee, Memphis	5/60	8.3	0/2	0.0	5/58	8.6
Oregon Health Science Center, Portland	2/27	7.4	1/4	25.0	1/23	4.4
University of Michigan, Ann Arbor	4/60	6.7	1/6	16.7	3/54	5.6
University of Ottawa, Canada	1/15	6.7	0/1	0.0	1/14	7.1
Loyola University, Maywood, IL	2/34	5.9	2/19	10.5	0/15	0.0
St. Louis University, MO	1/20	5.0	0/0	None	1/20	5.0
University of Pennsylvania, Philadelphia	2/43	4.7	0/6	0.0	2/37	5.4
Winthrop University, Mineola, SC	6/131	4.6	0/10	0.0	6/121	5.0
University of Utah, Salt Lake City	2/53	3.8	0/7	0.0	2/46	4.4
Beth Israel Hospital, Boston	3/84	3.6	0/3	0.0	3/81	3.7
Massachusetts General Hospital, Boston	6/173	3.5	0/8	0.0	6/165	3.6
University of California, San Diego	1/29	3.5	0/0	None	1/29	3.5
Cleveland Clinic, Cleveland, OH	1/32	3.1	0/2	0.0	1/30	3.3
University of California, Los Angeles	2/71	2.8	0/3	0.0	2/68	2.9
Toronto General Hospital, Toronto, Canada	2/139	1.4	0/9	0.0	2/130	1.5
Ohio State University, Columbus	1/89	1.1	0/4	0.0	1/85	1.2
Baylor College of Medicine, Houston, TX	0/8	0.0	0/7	0.0	0/1	0.0
Mt Sinai Hospital, New York	0/13	0.0	0/0	None	0/13	0.0
New York City College, New York	0/36	0.0	0/0	None	0/36	0.0
University of Nebraska, Omaha	0/19	0.0	0/0	None	0/19	0.0
University Hospital, London, Canada	0/1	0.0	0/1	0.0	0/0	None
University of Pittsburgh	0/25	0.0	0/0	None	0/25	0.0
Tulsa Heart Institute, OK	0/2	0.0	0/0	None	0/2	0.0
Minneapolis Heart Institute, MN	0/7	0.0	0/0	None	0/7	0.0
Total	59/1,355	4.4	6/102	5.9	53/1,253	4.2

+/Total = number of patients with positive HCV antibodies/number of patients studied at that institution.

significant. Cardiac troponin I tended to be higher in 6 patients with (2.5 ± 1.3) than in 53 patients without biopsy-proven myocarditis (1.8 ± 0.7 ng/mL, $P = .75$). Cardiac troponin T was similar in both groups (0.04 ± 0.02 versus 0.05 ± 0.01 ng/mL, $P = .84$).

The concentrations of NT-proBNP were elevated (≥55 pg/mL) in 42 of 42 patients (100%) with HCV antibodies, (10,000 ± 5860 pg/mL), a mean value significantly greater than in 1276 patients without HCV antibody (2508 ± 160 pg/mL, $P < .0001$).

Discussion

Evidence accumulated in the past few years indicates that the immune system clears the virus from the bloodstream during the initial infection in 15% to 25% of individuals infected with HCV, whereas in the remaining 75% to 85%, the disease becomes chronic. Hepatocytes killed by the HCV are replaced by fibrotic tissue, ultimately resulting in cirrhosis in 10% to 20%, or in hepatocellular carcinoma in 1% to 5% of chronically infected patients. However, the majority of patients develop none of these complications as late as 20 years after the onset of infection.[1] Approximately two thirds of patients suffer from minimal, nonspecific changes or from mild chronic persistent hepatitis, whereas approximately 20% develop chronic active hepatitis. Predictors of more severe or more rapidly progressive disease are older age, immunodeficiency, concurrent alcohol abuse, and certain HCV strains and high degrees of genetic heterogeneity.[27]

We were able to identify anti-HCV antibodies, HCV RNA, NT-proBNP, and cardiac troponin I and T in sera stored for up to 17 years and found the antibodies to be more prevalent in patients with myocarditis than in the general US population. The amounts of HCV RNA recovered varied widely among patients. Furthermore, whereas the prevalence of HCV infection in patients with active myocarditis and biopsy specimens that met the Dallas criteria tended to be higher than in patients without active myocarditis, the latter also had a higher prevalence of infection than the general population. It appears that, as observed with liver disease, the severity and time course of myocarditis associated with HCV infection is highly variable.

In an initial study, we evaluated 31 patients with cardiomyopathy and myocarditis by polymerase and found HCV RNA in 6 patients with dilated cardiomyopathy (19.4%).[17] In a collaborative research project of the Committees for the Study of Idiopathic Cardiomyopathy in Japan, HCV antibody was found in 42 of 663 patients with dilated cardiomyopathy (6.3%), significantly higher than the 2.4% prevalence in age-matched volunteer blood donors in Japan.[28]

Table 3. Quantification of Hepatitis C Virus RNA and Classification of Hepatitis C Virus, NT-proBNP, and Cardiac Troponin I and T in Sera of Patients With Positive Antibody Against Hepatitis C Virus

ProBNP (pg/mL)	Troponin-I (ng/mL)	Troponin-T (ng/mL)	HCV-RNA (kU/mL)	HCV group	Dx
217907	5.5	0.05	20	—	(−)
122766	1	0.27	560	1	(−)
20285	2.1	0.1	800	1	(−)
13692	0.3	0.08	130	1	(−)
8537	0.7	0	<0.5	—	(−)
4982	1.9	0.04	<0.5	1	(−)
3276	0	0	120	1	(−)
2570	35.3	0.58	<0.5	—	(−)
2499	0	0	<0.5	—	(−)
2455	5.4	0.1	130	1	(−)
1751	0	0	14	1	(+)
1713	0.4	0	15	1	(−)
1700	7.8	0.17	8.9	1	(−)
1563	1.5	0.04	<0.5	—	(−)
1558	1.1	0.03	210	1	(−)
1368	ND	0.06	<0.5	1	(−)
1168	0	0	<0.5	1	(−)
992	3	0.06	<0.5	—	(+)
940.1	0.6	0.38	210	1	(−)
881	0	0	120	1	(−)
854.1	0	0	130	1	(+)
838.2	1.4	0.01	150	1	(−)
680.2	0.3	0.04	<0.5	—	(−)
677.1	2	0	<0.5	1	(−)
633.9	0	0	<0.5	—	(−)
585.7	2.1	0.05	<0.5	1	(−)
528.4	1	0	51	1	(−)
493	1.5	0	26	1	(+)
477.6	8.3	0.12	<0.5	—	(+)
471.6	2.3	0.09	<0.5	2	(−)
471.1	0	0	1	1	(−)
413.2	0	0	<0.5	—	(−)
394.6	0	0.01	<0.5	—	(−)
391.6	ND	0	<0.5	1	(−)
373.3	1.3	0	8.9	—	(−)
325.5	0.4	0	170	1	(−)
224.2	2.6	0	410	1	(−)
223.9	0	0	1.9	—	(−)
196.7	0.5	0	<0.5	—	(−)
140.2	4	0.1	120	1	(−)
91.57	2.1	0	<0.5	—	(−)
59.86	1.6	0.02	18	2	(−)
ND	0.6	0	610	1	(−)
ND	0	0.01	230	—	(−)
ND	0	0	180	—	(−)
ND	0.2	0	110	1	(−)
ND	0.2	0	36	1	(−)
ND	2.4	0.09	6.5	1	(−)
ND	2.4	0.11	<0.5	—	(−)
ND	2.1	0	<0.5	—	(−)
ND	2	0.06	<0.5	—	(+)
ND	1.6	0.04	<0.5	—	(−)
ND	0.1	0	<0.5	—	(−)
ND	0	0.06	<0.5	1	(−)
ND	ND	0.04	<0.5	—	(−)
ND	0.3	0	<0.5	—	(−)
ND	0.2	0	<0.5	—	(−)
ND	0.1	0	<0.5	—	(−)
ND	0.1	0	<0.5	—	(−)

(−) = myocarditis absent; biopsy specimens satisfied Dallas criteria.
(+) = myocarditis present; biopsy specimens did not satisfy Dallas criteria.
ND = not done.

In a collaborative multicenter study conducted by the Scientific Council on Cardiomyopathies of the World Heart Federation, we recovered HCV genomes in the hearts from 2 of 11 patients with dilated cardiomyopathy and myocarditis from Italy (18%), and in the hearts of 4 of 11 patients from the US (36%), 2 of whom suffered from myocarditis and 2 from arrhythmogenic right ventricular cardiomyopathy.[22]

Okabe et al have reported the recovery of positive and negative strands of HCV RNA in paraffin-embedded cardiac tissue blocks from patients with chronic active myocarditis.[18] In a previous study, we found both β-actin gene and HCV RNA in a heart autopsied in 1979, confirming that HCV genomes are preserved for at least 19 years, and that HCV RNA can be detected in tissue specimens preserved for many years.[20] Both positive and negative strands of HCV genomes were detectable, suggesting that HCV replicates in the myocardium.

We also analyzed postmortem specimens from patients with dilated cardiomyopathy obtained from the University of Utah, and found HCV RNA in 8 of 23 hearts (35%) with positive actin genes.[22] However, there were wide variations in the rates of HCV genomes detection among different cities. HCV genomes were detected in none of 24 hearts from St. Paul's Hospital in Vancouver, Canada.[22] This suggests that the frequency of cardiomyopathy caused by HCV infection varies among different regions or different populations. A negative association between HCV infection and dilated cardiomyopathy has been reported by European investigators,[29,30] although these discordant results may be due to inappropriate controls, incomplete clinical investigations, or regional or ethnic differences.

Progress has been made recently in the identification of new serum markers of myocyte injury.[31] Cardiac troponin I, which regulates the calcium-mediated interaction between actin and myosin, is a sensitive and highly specific serum marker of cardiac injury.[32] Because most of the cardiac troponin I is physically associated with the myocyte contractile apparatus, it is released slowly into the serum and can be detected for up to 14 days after cardiac injury. This provides a wider window to detect cardiac injury than was previously available with markers such as creatine kinase-MB. In a previous substudy of the Myocardial Treatment Trial, cardiac troponin I was elevated in patients with myocarditis and its measurement identified reliably patients who had histologic findings consistent with this diagnosis.[33] In this study, elevated concentrations of cardiac troponin I and T were found in significant numbers of patients, suggesting the persistence of ongoing myocardial injury. Because the activity of antibodies against HCV and the structure of cardiac protein such as troponin I and T may be partly lost during prolonged storage, the true prevalence may be higher than measured in this study. High serum concentrations of cardiac troponin I and T are prognostic markers of poor prognosis in patients with heart failure.[34,35] Serial measurements of serum concentrations of cardiac troponins seem reliable to monitor myocyte injury, and

we have hypothesized that, in patients with cardiomyopathy and heart failure, therapeutic interventions which improve the long-term prognosis should be associated with a fall in cardiac troponin T. Increased concentrations of circulating NT-proBNP have been proposed as a marker of symptomatic cardiac dysfunction and a prognostic marker in heart failure,[36–38] and NT-proBNP has been shown to be the most sensitive marker of myocardial dysfunction and the most powerful prognostic factor in the specific form of cardiomyopathy from amyloidosis. In our study, NT-proBNP concentrations were increased in all patients with HCV antibody, and the increases were greater than in patients without HCV antibody. In patients with heart failure from HCV myocarditis, NT-proBNP is a more sensitive marker of myocardial injury than cardiac troponins.

Because NT-proBNP can be measured in serum as well as in plasma, the measurements of NT-proBNP can be performed more broadly in specimens from previous studies stored as sera instead of plasma. Measurements of a serum marker highly sensitive and specific for cardiac myocyte injury, such as NT-proBNP or cardiac troponin I or T, at the time of evaluation of patients with HCV infection may be an important first step toward the design of new methods to diagnose HCV-induced myocarditis.

Because HCV infection is a newly recognized and important cause of myocarditis, we propose the establishment of a collaborative global network to more precisely measure the prevalence of its cardiac involvement, and to conduct a therapeutic trial.

Acknowledgment

The authors would like to thank Abbott Laboratories for helping analyses of anti-HCV antibody and cardiac troponin I; Roche Diagnostics for helping analyses of NT-proBNP; and M. Shimada and M. Ozone for preparing the manuscript.

References

1. Cohen J. The scientific challenge of hepatitis C. Science 1999;285: 26–30.
2. Alter MJ, Kruszon-Moran D, Nainan OV, et al. The prevalence of hepatitis C virus infection in the United States, 1988 through 1994. N Engl J Med 1999;341:556–62.
3. Johnson RJ, Gretch DR, Yamabe H, et al. Membranoproliferative glomerulonephritis associated with hepatitis C virus infection. N Engl J Med 1993;328:465–70.
4. Nakamura K, Matsumori A, Kusano KF, et al. Hepatitis C virus infection in a patient with dermatomyositis and left ventricular dysfunction. Jpn Circ J 2000;64:617–8.
5. Sato Y, Takatsu Y, Yamada T, et al. Interferon treatment for dilated cardiomyopathy and striated myopathy associated with hepatitis C virus infection based on serial measurements of serum concentrations of cardiac troponin T. Jpn Circ J 2000;64:321–4.
6. Di Bisceglie AM, Hepatitis C. Lancet 1998;351:351–5.
7. Kim KS, Hufnagel G, Chapman NM, Tracy S. The group B coxsackieviruses and myocarditis. Rev Med Virol 2001;11:355–68.
8. Bowles NE, Ni J, Kearney DL, et al. Detection of viruses in myocardial tissues by polymerase chain reaction. Evidence of adenovirus as a common cause of myocarditis in children and adults. J Am Coll Cardiol 2003;42:466–72.
9. Kuhl U, Pauschinger M, Bock T, et al. Parvovirus B19 infection mimicking acute myocardial infarction. Circulation 2003;108:945–50.
10. Pankuweit S, Moll R, Baandrup U, Portig I, Hufnagel G, Maisch B. Prevalence of the parvovirus B19 genome in endomyocardial biopsy specimens. Hum Pathol 2003;34:497–503.
11. Kawai C, Matsumori A, Fujiwara H. Myocarditis and dilated cardiomyopathy. Annu Rev Med 1987;38:221–39.
12. Abelmann WH, Lorell BH. The challenge of cardiomyopathy. J Am Coll Cardiol 1989;13:1219–39.
13. Olinde KD, O'Connell JB. Inflammatory heart disease: pathogenesis, clinical manifestations, and treatment of myocarditis. Annu Rev Med 1994;45:481–90.
14. Matsumori A, Kawai C. An animal model of congestive (dilated) cardiomyopathy: dilation and hypertrophy of the heart in the chronic stage in DBA/2 mice with myocarditis caused by encephalomyocarditis virus. Circulation 1982;66:355–60.
15. Feldman AM, McNamara D. Myocarditis. N Engl J Med 2000;343: 1388–98.
16. Liu PP, Mason JW. Advances in the understanding of myocarditis. Circulation 2001;104:1076–82.
17. Matsumori A, Matoba Y, Sasayama S. Dilated cardiomyopathy associated with hepatitis C virus infection. Circulation 1995;92:2519–25.
18. Okabe M, Fukuda K, Arakawa K, Kikuchi M. Chronic variant of myocarditis associated with hepatitis C virus infection. Circulation 1997; 96:22–4.
19. Matsumori A, Ohashi N, Hasegawa K, et al. Hepatitis C virus infection and heart diseases. A multicenter study in Japan. Jpn Circ J 1998; 62:389–91.
20. Matsumori A, Yutani C, Ikeda Y, Kawai S, Sasayama S. Hepatitis C virus from the hearts of patients with myocarditis and cardiomyopathy. Lab Invest 2000;80:1137–42.
21. Matsumori A. Cardiomyopathies and heart failure. In: Matsumori A, editor. Biomolecular, infectious and immune mechanisms. Boston: Kluwer Academic Publishers; 2003. p. 1–15.
22. Matsumori A. Hepatitis C virus induces cardiomyopathies. Circ Res 2005;96:144–7.
23. Mason JW, O'Connell JB, Herskowitz A, et al. A clinical trial of immunosuppressive therapy for myocarditis. The Myocarditis Treatment Trial Investigators. N Engl J Med 1995;333:269–75.
24. Hahn EA, Hartz VL, Moon TE, et al. The Myocarditis Treatment Trial: design, methods and patients enrollment. Eur Heart J 1995; 16(Suppl O):162–7.
25. Aretz HT, Billingham ME, Edwards WD, et al. Myocarditis: a histopathologic definition and classification. Am J Cardiovasc Pathol 1987;1:3–14.
26. Tsukiyama-Kohara K, Yamaguchi K, Maki N, et al. Antigenicities of group I and II hepatitis C virus polypeptides—molecular basis of diagnosis. Virology 1993;192:430–7.
27. Hoofnagle JH. Hepatitis C: the clinical spectrum of disease. Hepatology 1997;26:15S–20S.
28. Matsumori A, Furukawa Y, Hasegawa K, et al. Epidemiologic and clinical characteristics of cardiomyopathies in Japan: results from nationwide surveys. Circ J 2002;66:323–36.
29. Dalekos GN, Achenbach K, Christodoulou D, et al. Idiopathic dilated cardiomyopathy: lack of association with hepatitis C virus infection. Heart 1998;80:270–5.
30. Prati D, Poli F, Farma E, et al. Multicenter study on hepatitis C virus infection in patients with dilated cardiomyopathy. North Italy Transplant Program (NITP). J Med Virol 1999;58:116–20.
31. Adams JE 3rd, Abendschein DR, Jaffe AS. Biochemical markers of myocardial injury. Is MB creatine kinase the choice for the 1990s? Circulation 1993;88:750–63.

32. Adams JE 3rd, Bodor GS, Davila-Roman VG, et al. Cardiac troponin I. A marker with high specificity for cardiac injury. Circulation 1993; 88:101–6.
33. Smith SC, Ladenson JH, Mason JW, Jaffe AS. Elevations of cardiac troponin I associated with myocarditis. Experimental and clinical correlates. Circulation 1997;95:163–8.
34. Sato Y, Yamada T, Taniguchi R, et al. Persistently increased serum concentrations of cardiac troponin T in patients with idiopathic dilated cardiomyopathy are predictive of adverse outcomes. Circulation 2001; 103:369–74.
35. Horwich TB, Patel J, MacLellan WR, Fonarow GC. Cardiac troponin I is associated with impaired hemodynamics, progressive left ventricular dysfunction and increased mortality rates in advanced heart failure. Circulation 2003;108:833–8.
36. Palladini G, Campana C, Klersy C, et al. Serum N-terminal pro-brain natriuretic peptide is a sensitive marker of myocardial dysfunction in AL amyloidosis. Circulation 2003;107:2440–5.
37. Hartmann F, Packer M, Coats AJ, et al. Prognostic impact of plasma N-terminal pro-brain natriuretic peptide in severe chronic congestive heart failure: a substudy of the Carvedilol Prospective Randomized Cumulative Survival (COPERNICUS) trial. Circulation 2004;110:1780–6.
38. Bettencourt P, Azevedo A, Pimenta J, Frioes F, Ferreira S, Ferreira A. N-terminal-pro-brain natriuretic peptide predicts outcome after hospital discharge in heart failure patients. Circulation 2004;110:2168–74.

臨　床

心臓移植

Heart transplantation

中谷武嗣
NAKATANI Takeshi

臓器移植

Key words　心臓移植　左心補助人工心臓　心筋生検

心臓移植は，従来の治療限界となった重症心不全を対象として，世界では6.6万例以上に施行され[1]，わが国では1997年10月に「臓器の移植に関する法律」が施行されてから35例に行われている[2]．2001年5月からは拡張型心筋症および拡張相肥大型心筋症に対する心臓移植手術が高度先進医療として承認され，本年4月からは健康保険において同種心移植術として移植関係学会合同委員会で心臓移植実施施設として選定された施設での実施が認められた．

心臓移植の適応

わが国での適応基準を表1に示す．適応となる主な疾患は，拡張型心筋症(DCM)および拡張相肥大型心筋症(dHCM)と虚血性心筋疾患で，心筋生検がDCMおよびdHCMの確定診断に必須である．適応検討においては，移植後免疫抑制療法が一生涯必要であることもあり，移植以外の治療手段，予測される余命，移植後の治療に対するコンプライアンスなどを含め表1の2，3で示す適応条件および除外条件を慎重に検討する．

適応決定と待機

わが国における心臓移植の適応決定は，現在各施設内適応検討会に加え日本循環器学会心臓移植適応検討小委員会の2段階審査で行われる(図1)[3]．この2段階審査において心臓移植の適応ありと判定されれば，各移植施設で本人および家族へのインフォームド・コンセントが行われ，諸手続きを経て日本臓器移植ネットワークの心臓移植待機リストへ登録し移植待機となる．現在，わが国での心臓移植は移植関係学会合同委員会で選定された7施設に限定されている．これまでに再移植申請2例を含む381例の申請があり，323例が適応と判定さている(表2)[4]．

移植待機中は，いつドナー情報が出ても移植できるように心不全治療を続ける．待機を続けているなかで心機能が改善し移植対象外となる症例や，あるいは感染や臓器障害などにより適応から外れる症例があるため，6ヵ月毎に再検討を行う．心不全が進行し重要臓器の機能障害を伴う症例では，心臓移植へのつなぎとして補助人工心臓(Ventricular Assist System：VAS)の適応を考慮する．現時点で用いられるVASには，体外設置型VASである東洋紡製国立循環器病セン

国立循環器病センター臓器移植部　部長

0371-1900/06/¥50/頁/JCLS

表1 心臓移植におけるレシピエント適応基準

1．適応となる疾患
心臓移植の適応となる疾患は，従来の治療法では救命ないし延命の期待がもてない以下の重症心疾患とする．
1)拡張型心筋症，および拡張相の肥大型心筋症
2)虚血性心筋疾患
3)その他(日本循環器学会および日本小児循環器学会の心臓移植適応検討会で承認する心臓疾患)
2．適応条件
1)不治の末期的状態にあり，以下のいずれかの条件を満たす場合
a)長期間またはくり返し入院治療を必要とする心不全
b)β遮断薬およびACE阻害薬を含む従来の治療法ではNYHA 3度ないし4度から改善しない心不全
c)現存するいかなる治療法でも無効な致死的重症不整脈を有する症例
2)年齢は60歳未満が望ましい
3)本人および家族の心臓移植に対する十分な理解と協力が得られること
3．除外条件
A)絶対的除外条件
1)肝臓，腎臓の不可逆的機能障害
2)活動性感染症(サイトメガロウイルス感染症を含む)
3)肺高血圧症(肺血管抵抗が血管拡張薬を使用しても6 wood単位以上)
4)薬物依存症(アルコール性心筋疾患を含む)
5)悪性腫瘍
6) HIV(Human Immunodeficiency Virus)抗体陽性
B)相対的除外条件
1)腎機能障害，肝機能障害
2)活動性消化性潰瘍
3)インスリン依存性糖尿病
4)精神神経症(自分の病気，病態に対する不安を取り除く努力をしても，何ら改善がみられない場合に除外条件となることがある)
5)肺梗塞症の既往，肺血管閉塞病変
6)膠原病などの全身性疾患

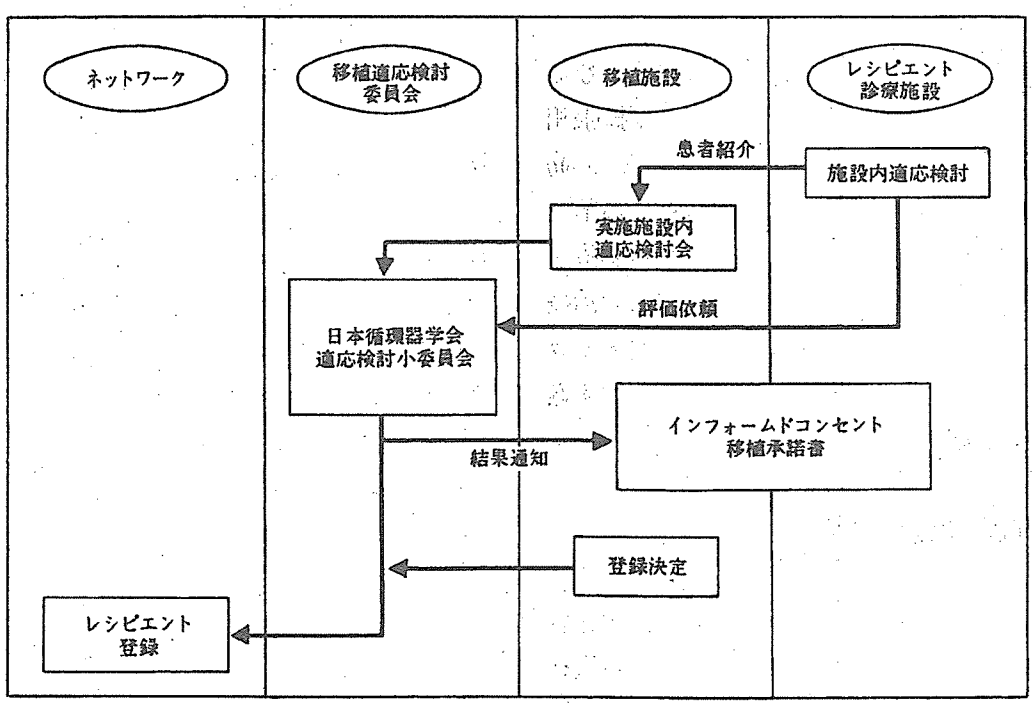

図1 レシピエントの申請・適応判定システム(文献3より)

表2 心臓移植適応検討に関する申請状況(1997年4月1日～2006年5月31日現在)(文献4より) (単位：名)

申請症例	379	検討中	0									
		検討症例	377	「適応」判定	321	15歳以上 277	待機中	31				
							ネットワーク登録	210	移植待機中	79		
									移植済	32	うち死亡	2
									登録取消	18		
									待機中死亡	81		
							死亡	15				
							海外移植済	21				
						15歳未満 44	待機中	26				
							ネットワーク登録	6	移植待機中	1		
									移植済	2		
									登録取消	2		
									待機中死亡	1		
							死亡	2				
							海外移植済	10				
				「再評価」判定	37	15歳以上 33	待機中	26				
							死亡	6				
							海外移植済	1				
						15年未満 4	待機中	3				
							死亡	1				
							海外移植済	0				
				「保留」判定	15	15歳以上 11	待機中	9				
							死亡	2				
							海外移植済	0				
						15歳未満 4	待機中	4				
							死亡	0				
							海外移植済	0				
				「不適応」判定	4	15歳以上		4				
						15歳未満		0				
		検討中死亡	2									
再移植申請	2	検討中	0									
		検討症例	2	「適応」判定	2	15歳以上	待機中	1				
							ネットワーク登録	1	移植待機中	1		
				「再評価」判定	0							
				「保留」判定	0							
				「不適応」判定	0							
		検討中死亡	0									

ター型(国循型)と埋め込み型左心補助人工心臓(LVAS)であるNovacor LVASがある[5].

2005年10月17日までの申請例における移植例をのぞく適応判定例およびネットワーク登録例の生存率を図2[3]に示すが，申請後2年で60%前後である．なお，多くの症例において申請時あるいは待機中に上記のLVASの適応が行われている．

ドナー心の評価とレシピエント候補の決定

まず，臓器移植のドナーとしての適否が検討され，全身性の活動性感染症やHIV抗体，HTLV-1抗体，HBs抗原，HCV抗体陽性などの陽性者，

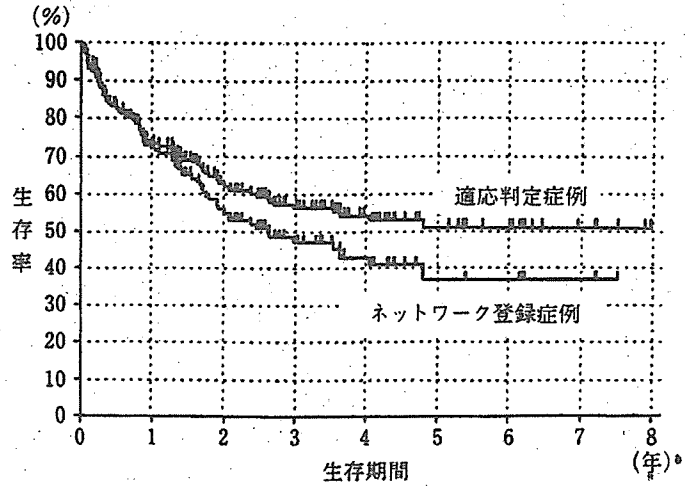

図2 適応と判定した症例およびネットワーク登録症例の Kaplan-Meier 生存曲線
(移植症例，移植後死亡症例を除く)(文献3より)

表3 わが国における心臓移植希望者(レシピエント)選択基準ー医学的緊急度

Status 1：次の(ア)から(エ)までの状態のいずれかに該当すること．
(ア)補助人工心臓を必要とする状態
(イ)大動脈内バルーンパンピング(IABP)を必要とする状態
(ウ)人工呼吸を必要とする状態
(エ)ICU，CCU 等の重症室に収容され，かつ，カテコラミン等の強心薬の持続的な点滴投与が必要な状態
Status 2：待機中の患者で，上記以外の状態
Status 3：Status 1，Status 2で待機中，除外条件(感染症等)を有する状態のため一時的に待機リストから削除された状態

クロイツフェルト・ヤコプ病およびその疑い，悪性腫瘍がある場合は該当しない．次いで心臓移植のドナーとしての検討がなされるが，心疾患，心臓外傷，開心術の既往があれば適さない．心臓移植のドナーとしての年齢は60歳以下が対象となるが，男性45歳，女性50歳以上では冠状動脈硬化性病変への配慮が必要となる．ドナー心の状態を心電図や心エコー図などで検討するとともに，カテコラミン剤が大量(ドパミン10μg/kg/min 相当以上)用いられている場合には心機能を慎重に検討する．最終判定は，ドナー手術において開胸下に触診および視診により冠動脈病変を含め心臓に異常がないことを確認して行う．

心臓移植のドナーとして初期情報で適当であると考えられる場合，日本臓器移植ネットワーク登録中の待機リストからレシピエント候補が選定される．適合条件は，血液型の一致あるいは適合，サイズの適合(体重差ー20～＋30％が望ましい)，前感作抗体がないこと(リンパ球・クロスマッチを実施)がある．適合条件に合致する複数の候補者がいる場合には，虚血許容時間(4時間以内に血流再開ができること)，医学的緊急度，ABO 式血液型および待機期間により優先順位を決定する．表3に医学的緊急度を示すが，status 1として補助人工心臓など循環呼吸補助を必要とする症例が優先される．血液型は一致が優先され，一致者がいなければ適合者に配分される．また，複数の同一条件患者がいる場合は長い待機期間者から優先される．

心臓移植手術[6]

いつドナー情報がもたらされるか予測できないため，常に短時間で準備ができる体制が必要である．さらに，心臓は他の臓器よりも許容虚血時間が短いため，ドナーチームとレシピエントチームの緊密な連係が重要である．

1. ドナー手術

ドナー手術において，開胸後の視診および触診によりドナー心臓の最終評価を行う．次いで，上行大動脈，肺動脈，上および下大静脈を剝離し，上行大動脈に心停止および保存液注入のカニューラを挿入し，他の臓器の準備が整うのを待つ．摘出予定臓器の準備が整った段階で，全身ヘパリン化を行い，上行大動脈に心停止および保存液注入用のカニューラを挿入する．同時に肺も摘出する場合は，肺動脈本幹に肺保存用カニューラが肺チームにより留置される．その後，肺チームにより肺動脈からプロスタグランディンE1を注入後，上大静脈を結紮する．次いで，上行大動脈を遮断し，心停止および保存液の注入を開始するとともに，下大静脈を遮断し切断する．Bicaval 法で行う場合には上および下大静脈長に注意が必要である．しかし，同時に肝臓が摘出される場合は，下大静脈の切断は右心房よりになる．肺静脈ー左房流入部を肺グループと調整しながら切離する．上大静脈を奇静脈直下で切断し，できるだけ長く上行大動脈を切断する．その後，左右肺動脈を分岐部で切断し，心臓を摘出する．摘出した心臓は，心保存液を満たしたビニール袋に入れたうえ，3重包装し，氷の入ったアイスボックスにて搬送する．心保存および停止液としては，種々のものが用いられるが，われわれは当初細胞外液型のSt.Thomas 液を用い，7例目からは心移植用に開発された1パック入りのCelsior 液に変更している．

2. レシピエント手術

レシピエント手術法には，心房位吻合を行うLower-Shumway 法と，上・下大静脈で吻合するbicaval 法があり，当センターではレシピエントの右房後壁の一部を温存して上・下大静脈で吻合するmodified bicaval 法を用いている[7]．まず，通常の心臓手術同様に胸骨正中切開にて心臓に到達する．左心補助人工心臓(LVAS)装着例では，高度の癒着があることが多く，さらに胸骨下にある送血側人工血管を損傷しないように注意する必要がある．なお，われわれはLVAS 装着手術において胸骨下を避けるように人工血管を留置し，さらにゴアテックスシートでカバーしている．ドナー心到着までに，上行大動脈および上下大静脈を剝離し，人工心肺の送血管および脱血管の挿入が行えるようにする．なお，LVAS 装着症例では人工血管吻合部も切除するために送血管を人工血管吻合部より末梢側で挿入する．送血管の挿入が困難な場合には，大腿動脈送血を行う．また，L字型の脱血管を用い，上大静脈上方および右房下大静脈連結部に挿入する．

ドナー心が到着してから体外循環を開始し，レシピエント心臓の摘出を行う．まず，右房壁を右房心耳付近から右房ー右室の房室間に沿って切開し，上方は大動脈根部へ下方は冠静脈洞に向けて切開する．大動脈を人工血管吻合部より末梢側で切断する．次いで，肺動脈を肺動脈弁直上で切断する．右房の切開を左房へ延長し僧帽弁を確認しながら弁直上付近で左房切開を行う．心房中隔壁をつけた状態で左房後壁側を残す．右房は，Lower-Shamway 法では冠静脈洞で切除する(図3[8]左)．Bicaval 法では右房壁をすべて除去する(図4[8]左)．modified bicaval 法では上大静脈および下大静脈間の後壁をストリップ状に残して切離し，心臓を摘出する(図5[6])．また，右上肺脈より左心ベントを挿入できるように準備しておく．なお，LVAS 施行例では，LVAS 駆動中止後大動脈遮断を行い，送血部の人工血管を遮断切離する．次いで，左室心尖部の脱血管をはずす．

搬送されたドナー心をバックテーブルにおいて，処理を行う．まず，ドナー心の左房の肺静脈間を切開してひとつの吻合口とする．左房より卵円孔を調べ，開存していれば閉鎖する．Lower-Shamway 法では，レシピエントの右房壁を下大静脈から右心耳にかけて切開する(図3中)．

ドナー心吻合は左心房から開始する．4-0プロリン糸を用い，ドナー心の左心耳下端がレシピエント心の左上および下肺静脈開口部の中央部に

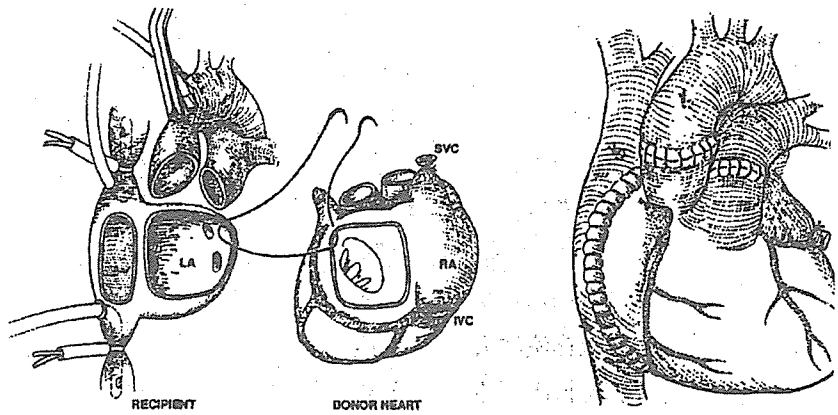

図3 Lower-Shamway 法(文献8より)

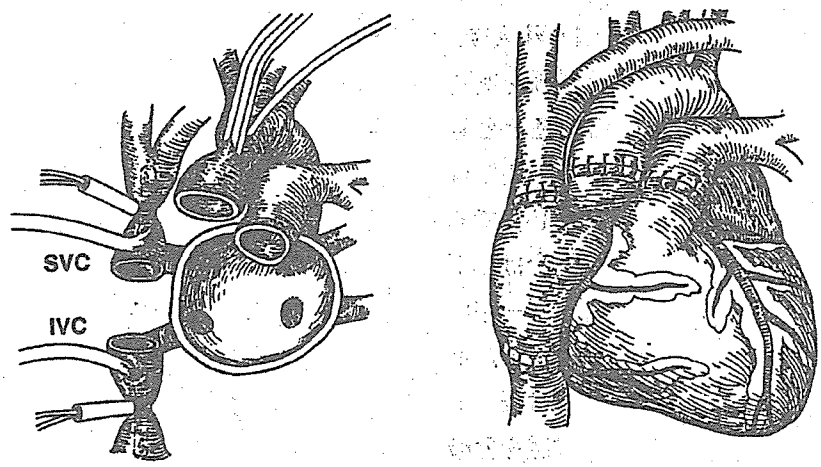

図4 Bicaval 法(文献8より)

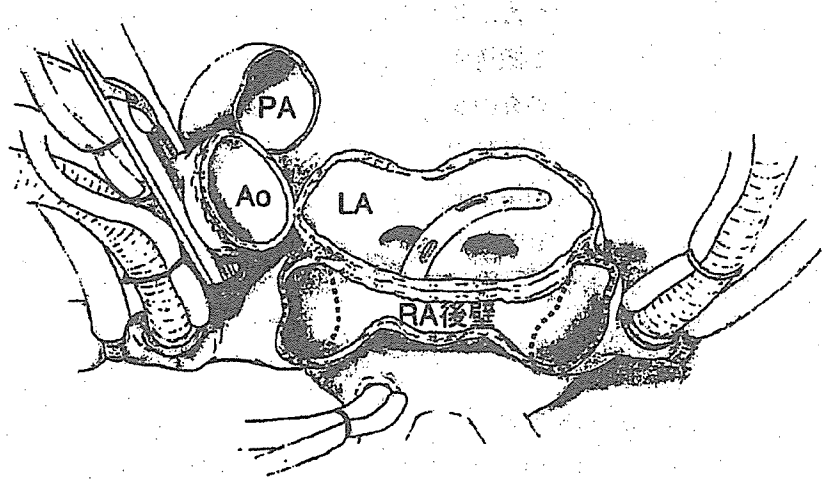

図5 Modified bicaval 法(文献6より)

くるように吻合を始める．Over and over suture で数針頭側へ運針した後，ドナー心を胸腔内に挿入する．ドナー心およびレシピエント心の左房部の口径差に注意しながら，左房吻合を続けるが，心房中隔左房側では，右房側を一緒に縫合する(図3中)．吻合終了前に左房ー僧帽弁を介して左室にベントチューブを挿入し，左室の充満を防ぐ．次いで，肺動脈をトリミングし4-0プロリン糸

にて連続吻合する．その後，4-0プロリン糸連続縫合にて大動脈吻合を行い，大動脈遮断を解除する．なお，大動脈遮断解除前に，順行性再灌流を白血球除去フィルターを用いたleucocyte-depleted warm cardioplegiaにより行う．遮断解除後心室細動であれば，DCにて洞調律にする．最後に右房の吻合に移る(図3右)．Bicaval法(図4右)およびmodified bicaval法ではドナーの上下大静脈を各々5-0プロリン糸にて連続吻合を行う．

少量のカテコラミン(ドパミン)で心臓の収縮力が回復した後に左室ベントチューブを抜去し，体外循環より離脱する．なお，除神経心であるため除脈をきたしやすく，心拍数をペーシングあるいはイソプロテレノールにより90～120/分に維持する．心臓移植手術時の免疫抑制療法としては，手術開始後と大動脈遮断解除前にメチルプレドニゾロン500mgを静注する．

なお，補助人工心臓装着例では，手術終了前に，VASのチューブ(体外設置型LVAS)あるいは血液ポンプ(埋込み型LVAS)を除去する．

心臓移植後の管理[9]

心臓移植後の予後に影響する重要な因子として，移植心不全，急性拒絶反応，感染症，悪性腫瘍，冠動脈病変がある．

1. 移植心不全

ドナー心の摘出時における強心薬の使用状況と心機能，心保存法，手術手技などが関係する．強心薬が使用されている場合や経過中に心停止がある場合のドナー心機能評価は，心電図や心エコーにより慎重に行う．心保存液としては，ドナー病院で用いやすいものであることも重要で，われわれは1パック包装のCelsior液を用いている．また，虚血時間の短縮に努めることが重要で，短時間での搬送が行えるように小型ジェット機やヘリコプターを積極的に用いる．

2. 急性拒絶反応

臓器移植においては，拒絶反応の制御が重要であり，心臓移植の成績が向上したのは，拒絶反応の診断法として内頸静脈からの心内膜心筋生検法が確立したことと，新たな免疫抑制剤が開発されたためである．とくに急性拒絶反応は，移植後1年以内の頻度が高い．また，拒絶反応があるにもかかわらず臨床的に無症状である場合が多い．このため，定期的に心内膜心筋生検を行い，国際心臓肺移植学会の基準(表4)により判定する[10]．

免疫抑制療法としては，シクロスポリン(ネオーラル)あるいはタクロリムス(プログラフ)，ミコ

表4 心筋生検における病理診断基準(国際心臓肺移植学会)

Grade	Nomenclature	所見
0	No Rejection	標本上に拒絶反応を思わせる所見を認めない．
1A	Focal, Mild Acute Rejection	血管周囲および間質に局所的な大型リンパ球浸潤を認めるが，心筋細胞傷害は認めない．
1B	Diffuse, Mild Acute Rejection	血管周囲および間質によりびまん性に大型リンパ球球浸潤を認めるが，心筋細胞傷害は認めない．
2	Focal, Moderate Acute Rejection	周囲とは比較的明瞭に境界される大型リンパ球の浸潤巣を一ケ所のみ認め，心筋細胞傷害とともに心筋層の構築の変化を伴っている．好酸球の浸潤を伴うこともある．
3A	Multifocal, Moderate Acute Rejection	Grade 2と同様の炎症細胞浸潤巣を2カ所以上で認める．
3B	Diffuse, Borderline Severe Acute Rejection	心筋細胞傷害を伴ったびまん性の炎症細胞浸潤をいくつかの生検標本で認める．大型リンパ球や好酸球の他に好中球を認めることもあるが，出血は通常認められない．
4	Severe Acute Rejection	大型リンパ球，好酸球，好中球を含む多様な炎症細胞がびまん性に浸潤し，心筋細胞傷害および心筋細胞壊死が常に認められる．出血，浮腫，血管炎も通常存在する．

フェノール酸モフェチル(セルセプト)とステロイド(プレドニン)の3者併用療法が一般的に用いられる[11]．また，移植後に腎機能障害を伴った場合には抗胸腺抗体として，モノクローナル抗体のOKT3あるいはポリクローナル抗体であるATGを用いた免疫抑制の導入が行われる．国際心臓肺移植学会の基準2あるいは3A以上の所見がある場合には治療が必要で，まずステロイドパルス療法を行う．パルス療法に抵抗性の場合には抗胸腺抗体による治療が必要となる．

3. 移植後冠動脈病変

従来慢性拒絶反応と呼ばれてきたものであるが，移植心冠動脈にびまん性の求心性内膜肥厚が進行する．移植心は徐神経されているため，虚血病変が進行しても胸痛を自覚せず，心原性ショックを突然発症したり，不整脈による突然死を引き起こすことがある．定期的な冠動脈造影と血管内超音波検査(IVUS)により，内膜肥厚の所見に留意する．移植後冠動脈病変はびまん性であるため，血行再建術の適応とならない場合が多く，重症例では再移植が必要となる．

移植後冠動脈病変は心臓移植後の長期成績に大きく関係しており，危険因子として，免疫に関連するものとして，T細胞の活性化，細胞性拒絶反応，細胞増殖，HLAミスマッチなどが，またその他の因子として，ドナー年齢，虚血再潅流障害，CMV感染症，高脂血症などの関与が検討されているが，まだその発生機序は十分に解明されていない．このため，発生機序の解明および治療法の開発に関する研究が精力的に進められ，最近移植後冠動脈病変発現を抑制する免疫抑制剤として，sirolimus(Rapamycine)やeverolimus(RAD)(Certican)が開発され，わが国への導入も検討されている．

4. 感染症

免疫抑制療法を強力に行う移植後1年以内の頻度が最も高い．術後1ヵ月以内は細菌感染症が多く，その後はサイトメガロウィルス(CMV)や単純ヘルペスウイルスなどの日和見感染が増加する．このCMV感染は，移植後冠動脈病変の危険因子とされており，早期発見および治療が予後に大きく影響する．

5. 悪性腫瘍

免疫抑制療法は心臓移植後一生涯続ける必要があるが，使用期間が長くなるにつれて悪性腫瘍発生の危険性が高まる．国際レジストリーでは移植後3～5年の死因の21%を占めており，とくに，悪性リンパ腫(Post transplant lymphoproliferative disorder：PTLD)と皮膚癌への注意が必要である．

6. 心臓移植患者の中・長期管理

心臓移植患者におけるQOLの維持と良好な予後を得るために移植後の中・長期管理において，免疫抑制薬による腎機能障害や糖尿病などの予防，移植後冠動脈病変の進展予防のための高血圧や高脂血症の予防および治療，感染症予防(とくにCMV感染，ヘルペス感染など)，悪性腫瘍の早期発見，ステロイド使用による骨粗鬆症の進展予防などへの配慮が重要である．

世界の成績[1]

2005年の国際心肺移植学会統計では，1982～2003年までに66,751例の心臓移植が行われ，1年生存率は80.8%で，50%の患者の生存期間は9.6年で，移植後1年生存した症例での50%生存期間は12年であった．なお，生存率は免疫抑制療法などの進歩により上昇し，1年生存率では1982～88年の77.5%から1999～2003年では84.5%となっている．また，生存率は移植後冠動脈病変などにより移植1年以後年間ほぼ直線的に約4%ずつ低下している．免疫抑制療法としては，サイクロスポリン(あるいはタクロリムス)，ミコフェノール酸モフェチル，プレドニンの三者併用療法が主に行

われているが，最近ではRapamycineの使用例が増加している．また，導入療法として，ATGやOKT3に加え，最近ではIL2receptor antagonistが使用されている．死亡原因は，急性期では移植心不全，急性拒絶反応が多く，1年以後では移植後冠動脈病変や悪性腫瘍が増加している．また，身体活動に関する移植後7年までの調査において，90%以上が活動制限なしの生活を送っている．

表5 日本臓器移植ネットワークへの登録症例(2006年5月1日現在)

心臓	
登録待機中	85例(Status 1：42例)
移植	34例
取消し	12例
死亡	83例
海外渡航移植	26例
登録者累計	240例

わが国における心臓移植の成績[2)]

本年5月までに日本臓器移植ネットワークへ240人が登録され，34例(14%)の心臓移植が実施されたが，83名(35%)が待機中に死亡した(表5)[12)]．

施行例は，本年6月に1例施行され計35例(表6)となったが，原疾患は拡張型心筋症や拡張相肥大型心筋症など大部分は非虚血性の心筋症で，国際レジストリーにおける虚血性および非虚血性心筋症がほぼ同数とは大きく異なっている[1)]．待機状態は全例Status 1で，27例(77%)は左心補助人工心臓(LVAS)装着例であった．移植待機日数は当初は比較的短期だったが，その後長期化し，現在ではStatus 1として平均695日で1年以上待機は27例(77%)に及んでいる．LVAS装着期間も長期化し，平均739日で，21例(78%)が1年以上であった．東洋紡一左室型が最も多く，最長例は1,443日に及んでいる．

移植後2例が死亡したが，7年以上経過例が3例あり，図6に示すように国際レジストリーに比べ良好な成績を示している．日常生活では，とくに大きな生活制限を認めておらず，良好なQOLを示している．

表6 わが国における心臓移植症例

移植症例数	35例
年齢	8－61歳
性別	男性：26例，女性：9例
原疾患	拡張型心筋症：25例，拡張相肥大型心筋症：6例
	薬剤性心筋症：1例，虚血性心筋疾患：1例
	心筋炎後心筋症：1例，先天性心疾患：1例
待機状況	Status 1：全例
	補助人工心臓装着：27例
	強心薬持続投与：8例
待機期間(status 1)	29～1,390日(695日)【27例】
補助人工心臓補助期間	21～1,443日(739日)【21例】
	(最長例：東洋紡－左室型)
	東洋紡-左房型：2例【1例】
	東洋紡-左室型：19例【15例】
	Novacor：2例【1例】
	HeartMate-IP：2例【2例】
	HeartMate-VE：2例【2例】
実施施設	国立循環器病センター：18例　大阪大：9例
	東京女子医大：3例　九州大：2例
	埼玉医大：1例　東北大：1例　東京大学：1例

()：平均　【】：1年以上例

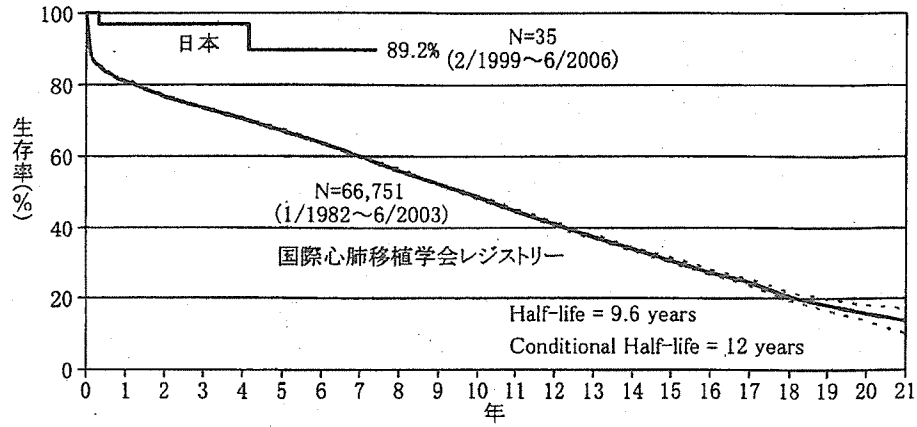

図6 心臓移植後の累積生存率

今後の展望

わが国での心臓移植施行例は少なく，全例がstatus 1でLVAS装着例が多く，待機期間も長期に及んでいる．しかし，移植後の成績は良好であり，わが国での心臓移植プログラムの充実が望まれる．

文　献

1) Taylor DO, Edwards LB, BOUCEK MM, et al：The registry of the International Society for heart and Lung Transplantation：Twentieth-second official adult heart transplant report-2005. J Heart Lung Transplant 24：945-955, 2005.
2) 中谷武嗣：臓器移植の現状と展望ー心臓および心肺移植．外科治療　94：50-56，2006.
3) 藤原久義，西垣和彦：なぜ内科医は移植医療にかかわらないか？ー心臓移植の立場からーわが国は信じがたい心臓移植後進国ー移植　41：2-9，2006.
4) 日本循環器学会 http://www.j-circ.or.jp
5) 中谷武嗣：治療の進歩：補助人工心臓．日本内科学会雑誌　94：111-118，2005.
6) 北村惣一郎：心臓移植．心臓血管外科手術書.ed. 小柳　仁，北村惣一郎，安井久喬．先端医療技術研究所．pp221-226，2002.
7) Kitamura S, Nakatani T, Bando K, et al：Modification of bicaval anastomosis technique for orthotopic heart transplantation. Ann Thorac Surg 72：1405-1406, 2001.
8) McCarthty PM, et al：Cardiac transplant admission, anesthsia, and operative proceudures. in The Stanford Mannual of Cardiopulmonary transplantation, Futura, New York, 1996.
9) 中谷武嗣，花谷彰久：心臓移植療法のパラダイムシフト．治療　86：2147-2155，2004.
10) 植田初江，由谷親夫，中谷武嗣：臓器移植の病理：心臓移植．移植　38：8-13，2003.
11) 中谷武嗣，花谷彰久，北村惣一郎：胸部移植プロトコール集．編集，北村惣一郎，黒澤博身，松田　暉他．メディカルビュー社，pp15-28，2003. 編集，北村惣一郎，黒澤博身，松田　暉他．メディカルビュー社，pp29-36，2003.
12) 日本臓器移植ネットワーク http://wwwjotnw.or.jp/

Overexpression of endothelial nitric oxide synthase accelerates atherosclerotic lesion formation in apoE-deficient mice

Masanori Ozaki,[1] Seinosuke Kawashima,[1] Tomoya Yamashita,[1] Tetsuaki Hirase,[1] Masayuki Namiki,[1] Nobutaka Inoue,[1] Ken-ichi Hirata,[1] Hiroyuki Yasui,[2] Hiromu Sakurai,[2] Yuichi Yoshida,[3] Masahiro Masada,[3] and Mitsuhiro Yokoyama[1]

[1]Division of Cardiovascular and Respiratory Medicine, Department of Internal Medicine, Kobe University Graduate School of Medicine, Kobe, Japan
[2]Department of Analytical and Bioinorganic Chemistry, Kyoto Pharmaceutical University, Kyoto, Japan
[3]Laboratory of Biochemistry, Faculty of Horticulture, Chiba University, Chiba, Japan

Nitric oxide (NO) derived from endothelial NO synthase (eNOS) is regarded as a protective factor against atherosclerosis. Therefore, augmentation of eNOS expression or NO production by pharmacological intervention is postulated to inhibit atherosclerosis. We crossed eNOS-overexpressing (eNOS-Tg) mice with atherogenic apoE-deficient (apoE-KO) mice to determine whether eNOS overexpression in the endothelium could inhibit the development of atherosclerosis. After 8 weeks on a high-cholesterol diet, the atherosclerotic lesion areas in the aortic sinus were unexpectedly increased by more than twofold in apoE-KO/eNOS-Tg mice compared with apoE-KO mice. Also, aortic tree lesion areas were approximately 50% larger in apoE-KO/eNOS-Tg mice after 12 weeks on a high-cholesterol diet. Expression of eNOS and NO production in aortas from apoE-KO/eNOS-Tg mice were significantly higher than those in apoE-KO mice. However, eNOS dysfunction, demonstrated by lower NO production relative to eNOS expression and enhanced superoxide production in the endothelium, was observed in apoE-KO/eNOS-Tg mice. Supplementation with tetrahydrobiopterin, an NOS cofactor, reduced the atherosclerotic lesion size in apoE-KO/eNOS-Tg mice to the level comparable to apoE-KO mice, possibly through the improvement of eNOS dysfunction. These data demonstrate that chronic overexpression of eNOS does not inhibit, but accelerates, atherosclerosis under hypercholesterolemia and that eNOS dysfunction appears to play important roles in the progression of atherosclerosis in apoE-KO/eNOS-Tg mice.

J. Clin. Invest. **110**:331–340 (2002). doi:10.1172/JCI200215215.

Introduction

Nitric oxide (NO), constitutively produced by endothelial nitric oxide synthase (eNOS), is a potent powerful vasodilator and possesses various vasoprotective effects such as inhibition of platelet aggregation, suppression of adhesion of leukocytes or monocytes on the endothelial surfaces, and inhibition of proliferation and migration of vascular smooth muscle cells. Because of these biological actions, eNOS-derived NO is regarded as an antiatherogenic factor. The observation of impaired endothelium-dependent vasorelaxation in hypercholesterolemia indicates that the loss of NO bioactivity is an early feature of atherosclerosis (1, 2). Therefore, preservation of NO bioactivity in the vessel walls might be one of the therapeutic strategies to inhibit the development of atherosclerosis. Indeed, administration of NO precursor L-arginine is demonstrated to restore the depressed endothelium-dependent vasodilatation in hypercholesterolemic rabbits and humans (3, 4). In addition, chronic administration of L-arginine is exhibited to cause the regression of preexisting intimal lesions through the restoration of NO bioactivity (5) and to inhibit the progression of atherosclerosis in cholesterol-fed rabbits and LDL receptor–deficient mice (6, 7). Therefore, upregulation of eNOS expression or restored NO bioactivity has been expected to inhibit the development of atherosclerosis.

Recently, the gene therapy of NOS was designed to increase or restore vascular NO production under the pathological situations in which the bioactivity of NO is reduced. In vivo gene transfer of eNOS or neuronal NOS is demonstrated to improve or augment NO-mediated vasorelaxation in atherosclerotic arteries (8). Furthermore, the gene transfer of eNOS could reduce

Received for publication February 6, 2002, and accepted in revised form June 3, 2002.

Address correspondence to: Seinosuke Kawashima, Division of Cardiovascular and Respiratory Medicine, Department of Internal Medicine, Kobe University Graduate School of Medicine, 7-5-1, Kusunoki-cho, Chuo-ku, Kobe, 650-0017, Japan.
Phone: 81-78-382-5842; Fax: 81-78-382-5859;
E-mail: kawashim@med.kobe-u.ac.jp.

Conflict of interest: No conflict of interest has been declared.

Nonstandard abbreviations used: nitric oxide (NO); endothelial nitric oxide synthase (eNOS); eNOS transgenic (eNOS-Tg); apoE-deficient (apoE-KO); tetrahydrobiopterin (BH_4); diaminofluorescein-2 diacetate (DAF-2 DA); 2-methyl-6-(4-methoxyphenyl)-3, 7-dihydroimidazol [1, 2-a] pyrazin-3-one-hydrochloride (MCLA); wild-type (WT); inducible NOS (iNOS).

adhesion molecule expression and inflammatory cell infiltration in carotid arteries of cholesterol-fed rabbits (9). Accordingly, the gene transfer of NOS has been expected as a favorable candidate of therapy for the prevention or inhibition of atherosclerosis. However, these beneficial effects are examined only in the short term by using a pharmacological approach or transient gene transfer. Furthermore, NOS itself produces superoxide anions in the absence of its substrate L-arginine or cofactors (10, 11). The long-term outcomes of gene delivery of NOS remain unclear, and its effects on vascular structures are undetermined. From these viewpoints, the actual roles of eNOS in the development of atherosclerosis should be examined by using the model that chronically overexpresses eNOS at the vessel walls.

In this study, we aimed to investigate the long-term effects of eNOS overexpression in the endothelium on the development of atherosclerosis by using genetically engineered mice. eNOS transgenic (eNOS-Tg) mice, which chronically overexpress eNOS in the vascular endothelium, show various vasoprotective effects on different vascular injury models by overproducing endothelium-derived NO (12–14). ApoE-deficient (apoE-KO) mice, a well-known animal model of atherosclerosis whose lesion development is similar to that observed in humans (15), were crossed with eNOS-Tg mice to generate eNOS-overexpressing apoE-KO (apoE-KO/eNOS-Tg) mice. We found promotion of atherosclerosis in apoE-KO/eNOS-Tg mice in comparison with apoE-KO mice, possibly due to the dysfunction of overexpressed eNOS in the endothelium that resulted in decreased NO bioactivity and enhanced production of superoxide. Supplementation with a NOS cofactor tetrahydrobiopterin (BH_4) reversed eNOS dysfunction and inhibited atherosclerotic progression. Our study provides evidence that the preservation of eNOS function rather than eNOS expression is essential for the prevention of atherosclerosis.

Methods

Materials. Diaminofluorescein-2 diacetate (DAF-2 DA) and 2-methyl-6-(4-methoxyphenyl)-3, 7-dihydroimidazol [1, 2-a] pyrazin-3-one-hydrochloride (MCLA) were purchased from Daiichi Pure Chemicals Co. (Tokyo, Japan) and Tokyo Kasei Kogyo Co. (Tokyo, Japan), respectively. Sapropterin hydrochloride, chemically synthesized BH_4, was obtained from Suntory Ltd. (Kyoto, Japan). The following Ab's were used: a rabbit polyclonal anti-eNOS Ab (Transduction Laboratories, Lexington, Kentucky, USA); a rat monoclonal anti-mouse monocyte/macrophage Ab (MOMA-2; Biosource International, Camarillo, California, USA); a monoclonal anti-α smooth muscle actin Ab (DAKO A/S, Glostrup, Denmark). All other chemicals were obtained from Sigma-Aldrich (St. Louis, Missouri, USA).

Animal preparation. Homozygous apoE-KO mice (50% C57BL/6J, 50% 129SVJ) (16) were backcrossed at least four times to C57BL/6J mice (93.8% C57BL/6J, 7.2% 129SVJ). eNOS-Tg mice (99.9% C57BL/6J) overexpressing bovine eNOS under the control of preproendothelin-1 promoter have been described previously (12). Heterozygous eNOS-Tg mice were crossed with apoE-KO mice to yield double-heterozygous mice (96.9% C57BL/6J, 3.1% 129SVJ). These heterozygous littermates were bred with apoE-KO mice to establish apoE-KO/eNOS-Tg mice. The animals used in this experiment were offspring of an intercross between apoE-KO/eNOS-Tg mice and apoE-KO mice (96.9% C57BL/6J, 3.1% 129SVJ). PCR was performed for genotyping for apoE (16) and the eNOS transgene (12).

Experimental design. ApoE-KO mice (n = 86) and apoE-KO/eNOS-Tg mice (n = 92) were weaned at 4 weeks of age onto a high-cholesterol diet (1.25% cholesterol, 7.5% cocoa butter, 7.5% casein, 0.5% sodium cholate; Oriental Yeast Co., Tokyo, Japan) (17) and maintained the diet for 8 or 12 weeks. In separate experiments, apoE-KO mice (n = 21) and apoE-KO/eNOS-Tg mice (n = 36) were maintained on a high-cholesterol diet supplemented with 10 mg/kg/day BH_4 as described previously (18). eNOS-Tg mice (99.9% C57BL/6J) were used in the experiments of immunoblotting for eNOS expression (n = 6) and NOS activity (n = 6). Their littermate wild-type (WT) mice were used for a control group in the experiments of immunoblotting for eNOS expression (n = 6), NOS activity (n = 6), and in situ superoxide detection (n = 14). Animals were provided the diet and water ad libitum and were maintained on a 12-hour light/dark cycle. All animal experiments were conducted according to the Guidelines for Animal Experiments at Kobe University Graduate School of Medicine.

Histological analysis of atherosclerotic lesions. The apoE-KO and apoE-KO/eNOS-Tg mice were euthanized at the age of 12 or 16 weeks, respectively (8 or 12 weeks on the high-cholesterol diet, respectively), and the atherosclerotic lesions were analyzed as described previously (19, 20). After mice were anesthetized with pentobarbital sodium (80 mg/kg intraperitoneally; Abbot Laboratories, Abbott Park, Illinois, USA), the aorta was perfused with normal saline containing 10 U/ml heparin. Then the aortic sample was dissected from the middle of left ventricle to the iliac bifurcation and fixed in 4% paraformaldehyde overnight. The samples were cut in the ascending aorta, and the proximal samples containing the aortic sinus were embedded in OCT compounds (Tissue-Tek; Sakura Finetechnical Co., Tokyo, Japan) and sectioned (10-μm thickness). Five consecutive sections, spanning 550 μm of the aortic root, were collected from each mouse and stained with Sudan III and Masson's trichrome. For quantitative analysis of the atherosclerosis, the total lesion area of five sections from each mouse was measured with the NIH 1.61 Imaging Software by modifying the method reported previously (17). The distal part of the excised aorta (from aortic arch to iliac bifurcation) was dissected free from surrounding tissues, opened longitudinally, and pinned onto a silicon-coated dish. Image analysis was performed on Sudan III–stained aortas with the NIH

1.61 Imaging Software. The amount of aortic lesion formation in each animal was measured as the percentage of lesion area per total area of the aorta (20).

Immunohistochemistry. Immunohistochemical staining for MOMA-2 and α-smooth muscle actin in atherosclerotic lesions in the aortic root were performed by the labeled streptavidin biotin method as described previously (12, 13). Quantitative analysis was shown as a percentage of the positive-stained area in the total atherosclerotic lesion area as described previously (21).

Hemodynamic analysis. Systemic blood pressure and heart rate were measured in WT, eNOS-Tg, apoE-KO, and apoE-KO/eNOS-Tg mice at 16 weeks of age under the conscious and unrestrained conditions as described previously (12). Blood pressure and heart rate were continuously measured and recorded on a Macintosh computer with MacLab system (Bioresearch Center, Nagoya, Japan) at least 4 hours after recovery from anesthesia.

Plasma lipid analysis. After mice were deprived of food for at least 12 hours, blood was collected by the cardiac puncture into heparin-coated tubes. Plasma was obtained through centrifugation of the blood for 15 minutes at 5,500 *g* at 4°C and stored at -80°C until each assay was performed. Concentration of total cholesterol and triglyceride were determined using an automated clinical chemistry analyzer. HDL-cholesterol levels were quantified by enzymatic reaction using a commercially available kit (Wako Pure Chemicals Industries, Osaka, Japan).

Protein analysis for eNOS. The protein samples were extracted from the mice at the age of 12 weeks. The expression of eNOS in aortas was analyzed by immunoblotting, and Ca^{2+}-dependent NOS enzymatic activity was determined by conversion of [^{3}H]-L-arginine to [^{3}H]-L-citrulline as described previously (12). Enzyme activity was expressed as citrulline production in picomoles per milligram of protein per minute.

In situ fluorescent signal detection and quantitative measurements of NO in aortas. NO production from aortas in situ was detected with fluorescence indicator DAF-2 DA (22–24). The fluorescent images of NO were obtained with a luminograph (LB981, NightOWL imaging system; EG&G Berthold, Bad Wildbad, Germany) as described previously (25). Briefly, the aorta containing aortic arch to iliac bifurcation was excised from 12-week-old animals, and adventitial tissues were dissected promptly in PBS (pH 7.4). The specimen was pinned onto a black-colored dish filled with 0.1 mol/l phosphate buffer (pH 7.4) containing 1.5 mmol/l calcium chloride and placed in a light-tight box to prevent interference by external light. DAF-2 DA was then added into the solution to yield the final concentration of 10 μmol/l. After 5 minutes of incubation, the sample was excited by blue light through the filter (485 nm). The emitted fluorescent image caused by the reaction of DAF-2 DA with NO was obtained by the luminograph with a band-pass filter (center of 532 nm), and its signal intensity was measured at the wavelength of 515 nm for 1 second. The aortic tissue was subsequently incubated in the presence of 1 μmol/l acetylcholine for 5 minutes, and the fluorescent signal image was again measured. After each experiment, the examined samples were stained with Sudan III to discriminate the atherosclerotic plaque from nonplaque areas.

The output data of fluorescent signal intensity due to NO was recorded and quantitatively analyzed by WinLight 32 software (the NightOWL-imaging system) for nonplaque areas of aorta. To exclude the interference of nonspecific emission and reflection from aortic collagen fibers, the background image was subtracted from each of the light-emission images after DAF-2 DA reaction. At least ten areas in the aorta (0.0005–0.001 cm^2) were randomly selected, and the fluorescent signals were measured in every area. The amounts of NO production were expressed as picowatts per centimeter square. NO production from the endothelium was estimated by subtracting the fluorescent signal under the basal condition from that under the acetylcholine-stimulated condition.

In situ detection and quantitative measurements of superoxide in aortas. Spatial distribution and quantitative determination of superoxide production was examined by chemiluminescent detection with a sensitive and specific probe, MCLA, which is a Cypiridina luciferin analogue (25–27). The chemiluminescent images were obtained by the NightOWL luminograph at the wavelength of 465 nm (25). Briefly, aortas excised from 12-week-old animals were dissected free from the surrounding tissues and mounted in a black-colored silicon dish filled with PBS at pH 7.4. After the samples were placed in a light-tight box to prevent interference by external light, MCLA was applied to the chamber (final concentration: 20 μmol/l). The light emission due to the in situ MCLA reaction with superoxide anion was measured for 5 minutes, and the measurement was repeated three times to confirm the reproducibility. The last signal image was used for the quantitative analysis. Subsequently, the endothelium was removed, and the chemiluminescent signal image was repeatedly obtained. The chemiluminescence due to superoxide was identified by application of Cu/Zn-SOD (400 U/ml) at the end of each measurement. The examined samples were then stained with Sudan III.

The output data of light emission was recorded as images of a nonlinear gray scale that were converted to the pseudocolor. The chemiluminescence signal intensities due to superoxide production were quantitatively analyzed with WinLight 32 software. Quantification of superoxide production was evaluated separately in approximately ten randomly selected sites (0.0012–0.002 cm^2) of either plaque or nonplaque area in aortic vessels that were discriminated by Sudan III staining. Measurements from each area were averaged in plaque or nonplaque area per animal after subtraction of the background signal. Quantification of superoxide production was expressed as the ratio (fold increase) to the average values obtained from WT mice. The reduced superoxide levels by endothelial

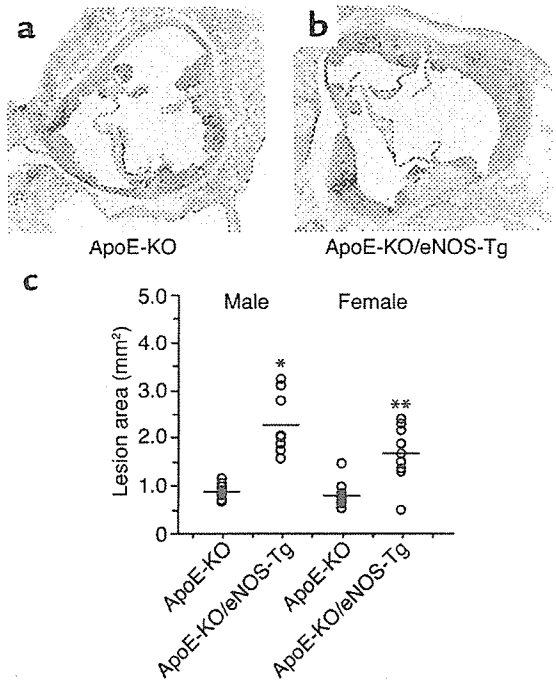

Figure 1
Atherosclerotic lesions in the aortic sinus. (**a** and **b**) Representative photographs of Sudan III–stained aortic root sections from apoE-KO and apoE-KO/eNOS-Tg mice fed on a high-cholesterol diet for 8 weeks. Sections were taken at the same level of aortic valves (original magnification ×15). (**c**) Quantitative analysis of atherosclerotic lesion size in males and females of apoE-KO and apoE-KO/eNOS-Tg mice. Total lesion area of five sections in the aortic root from each mouse was quantified morphometrically as described in Methods. Each symbol represents the lesion area measurement from an individual mouse, with the mean per group indicated by a horizontal line. After 8 weeks on a high-cholesterol diet, the atherosclerotic lesion areas were significantly increased in apoE-KO/eNOS-Tg compared with apoE-KO mice. $*P < 0.001$ vs. male apoE-KO mice; $**P < 0.01$ vs. female apoE-KO mice.

removal were expressed as a percentage of the reduced signal intensities to those before denudation.

BH_4 contents in aortas. Biopterin contents in aortas were measured by HPLC analysis as described previously (18, 28). The amount of BH_4 was calculated from the difference between the total (BH_4 plus BH_2 plus oxidized biopterin) and alkaline-stable biopterin (BH_2 plus oxidized biopterin).

Statistical analysis. Data were expressed as mean plus or minus SD. An unpaired Student *t* test was used to detect significant differences when two groups were compared. One-way ANOVA was used to compare the differences among three or four groups, with Bonferroni's test for post hoc analysis. *P* values less than 0.05 were considered statistically significant.

Results

Accelerated atherosclerosis by eNOS overexpression in apoE-KO mice. After 8 weeks on a high-cholesterol diet (at the age of 12 weeks), atherosclerotic lesion formation was observed in the aortic sinus of apoE-KO mice (Figure 1a). In apoE-KO/eNOS-Tg mice, unexpectedly, the atherosclerotic lesions were markedly promoted compared with apoE-KO mice (Figure 1b). As shown in Figure 1c, the lesion size was significantly increased 2.6-fold in male and twofold in female apoE-KO/eNOS-Tg mice compared with apoE-KO mice. In histological examination, the atherosclerotic plaque areas were remarkably greater in apoE-KO/eNOS-Tg mice than in apoE-KO mice (Figure 2). The percentage of MOMA-2–stained area in the plaque was not significantly different between the two groups (apoE-KO mice: 64% ± 14%; apoE-KO/eNOS-Tg: 61% ± 12%, *P* = NS). The α-smooth muscle actin–positive cells were few or hardly detectable (data not shown), and fibrotic changes were only partly distributed in the plaque lesions of both apoE-KO and apoE-KO/eNOS-Tg mice (Figure 2, c and d). Thus, the atherosclerotic lesions were more extended in apoE-KO/eNOS-Tg mice, whereas the cellular composition was not changed between the two groups.

The mean lesion areas in the aortic tree statistically did not differ between apoE-KO and apoE-KO/eNOS-Tg mice after 8 weeks on a high-cholesterol diet (percentage of lesion area: 8.8% ± 3.0% in male apoE-KO mice; 10.4% ± 2.4% in male apoE-KO/eNOS-Tg; 8.3% ± 2.8% in female apoE-KO mice; 10.8% ± 2.3% in female apoE-KO/eNOS-Tg; *P* = NS). For this reason, we extended the cholesterol feeding period for an additional 4 weeks. After 12 weeks on a high-cholesterol diet, the lesion formation in the aortic tree was also markedly progressed in apoE-KO/eNOS-Tg mice compared with apoE-KO mice (Figure 3, a and b).

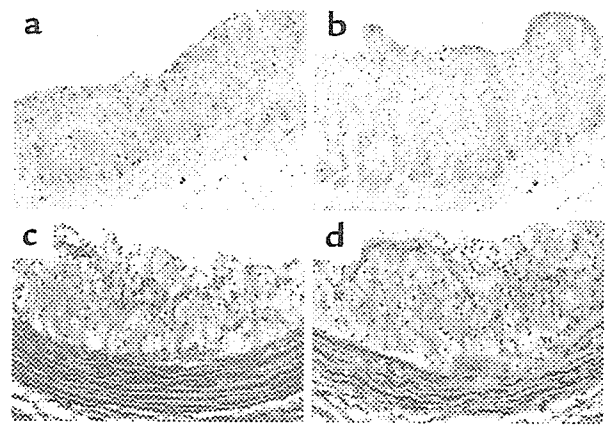

Figure 2
Histological examination of atherosclerotic lesions in the aortic root. (**a** and **b**) Photographs are representative of immunostaining for MOMA-2 in the atherosclerotic lesions, which showed no difference in the distribution between apoE-KO (**a**) and apoE-KO/eNOS-Tg mice (**b**) fed on a high-cholesterol diet for 8 weeks. (**c** and **d**) Fibrotic changes were detected with Masson's trichrome in the aortic root sections from apoE-KO (**c**) and apoE-KO/eNOS-Tg mice (**d**) fed a high-cholesterol diet. Fibrosis was only partly distributed in the plaque lesions of both mice (original magnification ×75).

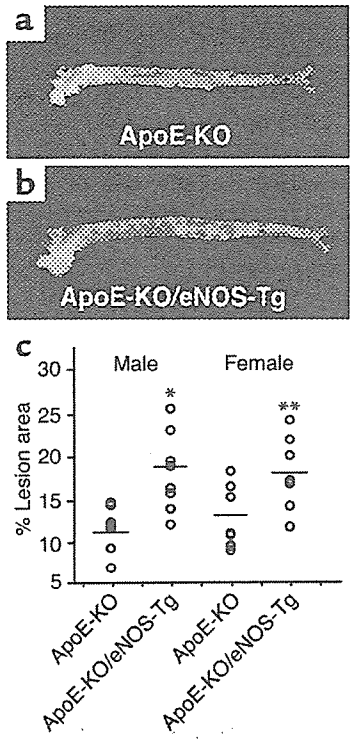

Figure 3
Atherosclerotic lesions in aortas. (**a** and **b**) Sudan III–stained, longitudinally opened aortas from apoE-KO (**a**) and apoE-KO/eNOS-Tg mice (**b**) at the age of 16 weeks. (**c**) Quantitative analysis of atherosclerotic lesion size in 16-week-old mice. After 12 weeks on a high-cholesterol diet, the lesion size in apoE-KO/eNOS-Tg mice was significantly greater than that in apoE-KO mice. Percentage of lesion area is the lesion area per total area of aorta. $*P < 0.0001$ vs. apoE-KO males; $**P < 0.001$ vs. apoE-KO females.

The quantitative analysis showed significant increases in the lesion area of 1.5 times in males and 1.4 times in females compared with apoE-KO mice (Figure 3c). Thus, atherosclerotic development was significantly accelerated by eNOS overexpression in the endothelium in the early stage of atherosclerosis.

Plasma lipids levels and hemodynamics. Plasma cholesterol levels were remarkably elevated by a high-cholesterol feeding in both apoE-KO and apoE-KO/eNOS-Tg mice; however, there was no significant difference between the two groups (Table 1). In contrast, triglyceride levels were not affected by a high-cholesterol diet in both groups (Table 1). Mean systemic blood pressure in apoE-KO/eNOS-Tg mice was 83.2 ± 7.4 mmHg ($n = 8$), which was approximately 20 mmHg lower than that in apoE-KO mice (103.5 ± 5.6 mmHg; $n = 7$, $P < 0.01$). As reported previously (12), eNOS overexpression in the endothelium significantly decreased blood pressure in apoE-KO mice.

Expression of eNOS and NOS activity in aortas. As shown in Figure 4, a and b, eNOS expression in aortas from eNOS-Tg mice was significantly greater than in WT mice. The protein levels of eNOS in apoE-KO/eNOS-Tg mice were also 10.8 times and 3.6 times greater than in WT mice and apoE-KO mice, respectively. Interestingly, in accordance with the report of Laursen et al. (29), each protein level of eNOS in apoE-KO or in apoE-KO/eNOS-Tg mice was slightly, but significantly, increased compared with WT or eNOS-Tg mice, respectively.

Ca^{2+}-dependent NOS activity in aortas was 1.8 times higher in eNOS-Tg mice than in WT mice (eNOS-Tg: 2.73 ± 0.61 pmol/mg protein/min vs. WT: 1.51 ± 0.12 pmol/mg protein/min; $P < 0.05$, $n = 6$ for each group). ApoE-KO/eNOS-Tg mice also showed a significant increase in NOS activity compared with apoE-KO mice (apoE-KO/eNOS-Tg: 3.05 ± 0.31 pmol/mg protein/min vs. apoE-KO: 2.10 ± 0.51 pmol/mg protein/min; $P < 0.05$, $n = 6$ for each group). However, NOS activity in apoE-KO/eNOS-Tg mice did not differ from that in eNOS-Tg mice.

NO production in aortas. The fluorescent signal intensities due to acetylcholine-stimulated NO production were not significantly different between WT and apoE-KO mice (WT mice: 35,680 ± 8,920 pW/cm^2, apoE-KO mice: 32,330 ± 3,890 pW/cm^2; P = NS). In apoE-KO/eNOS-Tg mice, the endothelium-derived NO production was 1.5 times higher than that in apoE-KO mice (Figure 4, c–g). However, the NO bioactivity in apoE-KO/eNOS-Tg mice was relatively lower than that assumed from the increase in eNOS protein levels.

Increased superoxide production in aortas from apoE-KO/eNOS-Tg mice. To investigate the spatial distribution and the quantitative determination of superoxide production in the atherosclerotic vessels, in situ superoxide detection was performed with MCLA. As shown in Figure 5, a and d, the chemiluminescent signal due to superoxide production was hardly detectable in aortas from WT mice. On the other hand, the clear chemiluminescent signal was detected in the atherosclerotic

Table 1
Plasma lipids in apoE-KO mice and apoE-KO/eNOS-Tg mice

		WT (C57BL/6)	ApoE-KO		ApoE-KO/eNOS-Tg	
			Male	Female	Male	Female
Number		7	7	6	8	7
T-CHO	mg/dl	64.0 ± 9.0	2059.8 ± 89.3[A]	1959.3 ± 94.3[A]	1841.0 ± 81.4[A]	1981.7 ± 55.4[A]
HDL-C	mg/dl	31.6 ± 4.3	66.2 ± 15.2	43.2 ± 9.9	61.8 ± 11.1	45.7 ± 11.3
Triglyceride	mg/dl	9.2 ± 1.2	6.2 ± 1.5	7.5 ± 1.0	3.8 ± 0.8	11.0 ± 1.7

ApoE-KO and apoE-KO/eNOS-Tg mice were fed on a high-cholesterol diet for 8 weeks. Animals were fasted for at least 12 hours and bled, and plasma total cholesterol, HDL cholesterol, and triglycerides were determined as described in Methods. [A]$P < 0.01$ vs. WT mice. T-CHO, plasma total cholesterol; HDL-C, HDL cholesterol.